Tracking and Transmission Design in Terahertz V2I Networks

Zheng Lin, Lifeng Wang, *Member, IEEE*, Jie Ding, *Member, IEEE*,
Yuedong Xu, *Member, IEEE*, and Bo Tan, *Member, IEEE*

***Abstract*—This paper designs the vehicle tracking and resource allocation in the terahertz (THz) vehicle-to-infrastructure communications (V2I) networks, where roadside units (RSUs) equipped with leaky-wave antennas help to estimate the driving states of multiple vehicles and optimize the transmit power and bandwidth per vehicle after receiving the vehicles' feedback. Different from the conventional phased arrays, the leaky-wave antenna has the potential of improving the sensing accuracy with lower system overhead thanks to its unique spatial-spectral coupling feature. The generalized mobile scenario is studied in which vehicles drive at time-varying speeds. A novel unscented Kalman filter (UKF) based solution is proposed to track the vehicles without requirement of addressing the Doppler effect. Based on the estimated states of multiple vehicles, a low-complexity resource allocation method is developed to maximize the sum rate under user fairness concern. Simulation results confirm that the proposed tracking solution can evaluate the propagation angle, vehicle's states and inter-vehicle distance accurately, and the tailored resource allocation method strikes a delicate balance between the sum rate and user fairness in the multi-vehicle V2I scenario.**

***Index Terms*—Terahertz V2I, leaky-wave antenna, unscented Kalman filter, resource allocation.**

I. Introduction

Vehicle-to-infrastructure communications (V2I) play an essential role in supporting vehicle-to-everything (V2X) services [2] and intelligent transportation systems (ITS) [3–5]. The V2I-aided sensing and communication can assist robust automated driving with extended sensors [6]. With the development of 5G millimeter wave (mmWave) technology, vehicle positioning via mmWave V2I has been studied in vehicular networks [7–9]. Since THz transmission is one of 6G potential technologies [10–12], terahertz (THz) V2I with much wider channel bandwidths enable higher sensing accuracy and lower-latency communication than mmWave V2I [10, 13].

In THz systems, selecting an appropriate type of antenna is crucial [12]. Although phased arrays have been used in 5G mmWave systems, the implementation of them in the THz links are confronted with many challenging issues involving antenna scale [10, 14], path discovery [15], feed network design [16] and beam squinting [17], etc. Moreover, extensive beam training is required for phased arrays in the 5G mmWave setup, which may result in much higher latency in the THz systems [11]. Compared to the conventional phased arrays, easy-to-manufacture leaky-wave antennas are envisioned as a promising approach to establish cost-effective THz links [16, 18, 19]. The applications of leaky-wave antennas have been considered in many areas such as THz radar sensing [20, 21] and THz frequency-division multiplexing communication [22] etc. One big characteristic of the leaky-wave antenna is that frequencies are coupled with the propagation angles, which can be exploited for designing more efficient path discovery and mobile object tracking [15, 23]. Based on this characteristic, a roadside unit (RSU) equipped with one single leaky-wave antenna can simultaneously estimate the inter-vehicle distance in multi-vehicle systems which have the capabilities of the adaptive cruise control (ACC) and cooperative ACC (CACC) [5, 24]. In addition, differing from the beam management in the phased array systems [25], exhaustive beam scanning is unnecessary in the leaky-wave antenna systems as demonstrated in [15, 23]. Therefore, the use of leaky-wave antennas brings the great potential for improving sensing and communication efficiency in the THz V2I networks.

Channel tracking designs in the mmWave and THz cellular systems have been investigated in the literature [26–30]. It is shown in [26] that the extended Kalman filter (EKF) can be a low-complexity tracking filter in mmWave mobile environments. Meanwhile, an EKF-based tracking strategy is proposed to minimize the beam alignment error of the mmWave systems in [27]. The work of [28] focuses on the direction of arrival tracking with unscented Kalman filter (UKF) in the mmWave massive multiple-input multiple-output (MIMO) cellular systems, where a kinematic model of the direction of arrival is considered and the rotated spatial support indexes are the observations. To make fast THz channel tracking in the linear user motion model, [29] attempts to estimate the propagation angle with the assistance of the prior beamspace channel information in the THz massive MIMO cellular systems with conventional antenna arrays. In [30], a beam zooming based wideband beam tracking is developed to simultaneously track multiple user physical directions, and the beam squinting effect is flexibly controlled, in this way, the beam training overhead can be significantly reduced. The application of dual-functional radar-communication (DFRC) technique in the mmWave V2I networks is considered in [9], where an EKF based beam tracking scheme is proposed by addressing the case of vehicle driving at constant speed.

Resource allocation also plays an important role in the THz systems. In [31], THz bandwidth allocation is studied in the

Manuscript received October 9, 2021; revised July 2, 2022; accepted September 29, 2022. This work was supported in part by the National Key Research and Development Program under Grant 2021YFE0193300, in part by the National Science Foundation of China (NSFC) under Grant 62002065, and in part by the Science and Technology Commission of Shanghai Municipality (STCSM) under Grant 22QA1401100. The work of Bo Tan was supported in part by the Academy of Finland under the project ACCESS (339519). This article was presented in part at the IEEE International Conference on Communications, 2022 [1]. The associate editor coordinating the review of this article and approving it for publication was M. Guillaud. *(Corresponding author: Lifeng Wang.)*

Z. Lin, L. Wang, J. Ding and Y. Xu are with the Department of Electrical Engineering, Fudan University, Shanghai, China (E-mail: {lifengwang, dingjie, ydxu}@fudan.edu.cn).

B. Tan is with the Faculty of Information Technology and Communication Sciences, Tampere University, Finland (E-mail: bo.tan@tuni.fi).

point-to-point THz system without addressing the mobility issues. Recent work [32] considers a random waypoint mobile model and analyzes the average bit error rate for the random and distance-aware bandwidth allocation methods in the THz-based subcarrier index modulation systems. A comprehensive overview of spectrum and power allocation schemes is provided in [33], where various designs are investigated in the THz systems with phased arrays.

Owing to the fact that THz channel tracking and resource allocation in the V2I networks is still in its infancy, this paper considers a generalized V2I scenario where vehicles drive at time-varying speeds, which has not been conducted yet. We develop a novel vehicle tracking method based on the THz V2I link with leaky-wave antenna. In such a significantly non-linear dynamic scenario, the EKF that adopts the first-order Taylor expansion for linearization [34] can lead to large estimation errors. The UKF amends the flaw of EKF by using a deterministic sampling approach while keeping the same computational complexity as the EKF [35–37]. Therefore, the main contributions of this paper are concluded as follows:

- In the considered THz V2I network, we design an UKF-based approach such that an RSU equipped with a single leaky-wave antenna can track multiple vehicles and their inter-vehicle distances. Different from the kinematic models seen in the existing works, we consider the generalized V2I networks in which vehicles can drive at non-linear time-varying speeds. The designed vehicle tracking method is robust and insensitive to the Doppler shift compared to the tracking method with conventional phased arrays, since phase information is not required. As such, the proposed design has much lower computational complexity with fast Kalman filter gain calculation, compared with the existing KF-based schemes.
- After estimating the V2I channel and inter-vehicle distance, a low-complexity resource allocation method is developed to maximize the sum rate under user fairness concern in the V2I networks with multiple vehicles. Different from the existing works, we show that inter-vehicle distance also has an effect on the bandwidth allocation in the dynamic V2I networks, due to the spatial-spectral coupling feature of the leaky-wave antenna.

The rest of this paper is organized as follows. The system model is described in Section II. The vehicle tracking solution is designed in Section III, and a user fairness aware resource allocation is proposed in IV. Section V covers the simulation results. Finally, some concluding remarks are presented in Section VI.

Notations: In this paper, $\mathrm{sinc}\,(x) = \sin(x)/x$ and $\mathrm{arccot}\,(x)$ is the inverse of cotangent function; $\mathbb{E}\{\cdot\}$ is the expectation operator; $(\cdot)^T$ is the transpose operator; $\mathrm{diag}\,(V)$ denotes the diagonal matrix whose diagonal elements are the entries of a vector V; $\mathbf{A}^{-1}$ is the inverse of the matrix $\mathbf{A}$.

II. System Descriptions

In the THz V2I network, the RSU equipped with a lowest transverse-electric (TE_1) mode leaky-wave antenna tracks multiple vehicles located in an arbitrary lane and each vehicle has one omnidirectional antenna. Based on [38], the far-field radiation pattern of TE_1 mode leaky-wave antenna can be calculated as

$$G\left(f,\theta\right)=\ell\mathrm{sinc}\left[\left(-j\alpha-k_0\left(f\right)\cos\theta+\beta\left(f\right)\right)\frac{\ell}{2}\right], \quad (1)$$

where f is the THz frequency, θ is the propagation angle ($0<\theta<90^o$), ℓ is the aperture length, $j=\sqrt{-1}$, α is the attenuation coefficient due to the power absorption in the structure, $k_0\left(f\right)=2\pi f/c$ with the speed of light c is the wavenumber of the free-space, $\beta\left(f\right)=k_0\left(f\right)\sqrt{1-\left(\frac{f_{\mathrm{co}}}{f}\right)^2}$ is the phase constant of the TE_1 mode based traveling wave, in which $f_{\mathrm{co}}=\frac{c}{2L}$ with the inter-plate distance L is the cutoff frequency. Given a line-of-sight (LoS) direction θ of a vehicle, the maximum level of the radiation can be obtained by using the frequency as follows [39]:

$$f^{\max}\left(\theta\right)=\frac{f_{\mathrm{co}}}{\sin\theta}, \quad (2)$$

in other words, the frequency $f^{\max}\left(\theta\right)$ needs to be chosen in order to achieve the maximum level of the radiation at the direction θ. As shown in the following section, such a spatial-spectral coupling feature for leaky-wave antenna can be leveraged to improve the efficiency of vehicle tracking, due to the fact that the vehicles are spatially separated in practice.

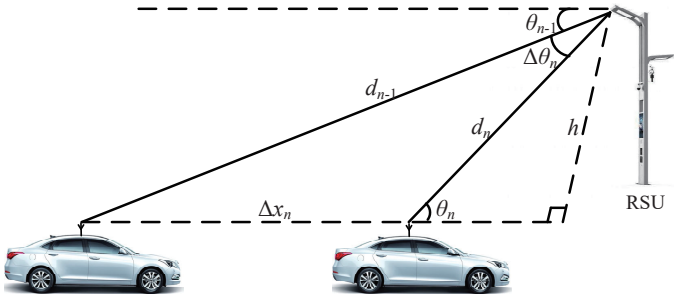

Fig. 1. An illustration of vehicle tracking.

Since each vehicle's states are estimated in the same fashion, we focus on an arbitrary vehicle for simplicity. As illustrated in Fig. 1, the geometric properties of a vehicle at the time $n-1$ and n are characterized as

$$\frac{h}{\sin\theta_{n-1}\sin\theta_n}=\frac{d_n}{\sin\theta_{n-1}}=\frac{d_{n-1}}{\sin\theta_n}=\frac{\Delta x_n}{\sin\Delta\theta_n}, \quad (3)$$

where h is the minimum communication distance and depends on the absolute antenna elevation difference and perpendicular distance between a vehicle in a lane and the RSU, θ_{n-1} and θ_n are the propagation angles, d_n and d_{n-1} are the communication distances at time n and $n-1$, respectively, $\Delta\theta_n=\theta_n-\theta_{n-1}$, and Δx_n is the moving distance from the time $n-1$ to n, which is calculated as

$$\Delta x_n=v_{n-1}\Delta\mathrm{T}+\frac{1}{2}a_{n-1}(\Delta\mathrm{T})^2. \quad (4)$$

In (4), v_{n-1} is the vehicle's velocity at the time $n-1$, $\Delta\mathrm{T}$ is the duration from the time $n-1$ to n, a_{n-1} is the acceleration/decelelation value at the time $n-1$, which is

assumed to be at least constant in a time interval (ΔT) [1]. We first derive the dynamics of the angle of departure, based on (3), we have

$$\frac{d_{n-1}}{\sin\Delta\theta_n\cos\theta_{n-1}+\cos\Delta\theta_n\sin\theta_{n-1}}=\frac{\Delta x_n}{\sin\Delta\theta_n}. \quad (5)$$

After some manipulations, (5) is re-written as

$$\Delta\theta_n=\operatorname{arccot}\left(\frac{d_{n-1}}{\Delta x_n\sin\theta_{n-1}}-\cot\theta_{n-1}\right). \quad (6)$$

Since $d_n=\frac{\Delta x_n\sin\theta_{n-1}}{\sin\Delta\theta_n}$ and $\sin\Delta\theta\approx\Delta\theta_n$ with small $\Delta\theta_n$, d_n can be approximated as

$$d_n\approx\frac{\Delta x_n\sin\theta_{n-1}}{\Delta\theta_n}=\frac{\Delta x_n\sin\theta_{n-1}}{\operatorname{arccot}\left(\frac{d_{n-1}}{\Delta x_n\sin\theta_{n-1}}-\cot\theta_{n-1}\right)}. \quad (7)$$

In light of (4), (6) and (7), the dynamical model for state evolution over the time is written as follows:

$$\begin{cases} v_n = \quad v_{n-1}+a_{n-1}\Delta\mathrm{T}+u_v, \\ \theta_n=\theta_{n-1}+\operatorname{arccot}\left(\frac{(\sin\theta_{n-1})^{-1}d_{n-1}}{v_{n-1}\Delta\mathrm{T}+\frac{1}{2}a_{n-1}(\Delta\mathrm{T})^2}-\cot\theta_{n-1}\right)+u_\theta, \\ d_n=\frac{\left(v_{n-1}\Delta\mathrm{T}+\frac{1}{2}a_{n-1}(\Delta\mathrm{T})^2\right)\sin\theta_{n-1}}{\operatorname{arccot}\left(d_{n-1}\left(\left(v_{n-1}\Delta\mathrm{T}+\frac{1}{2}a_{n-1}(\Delta\mathrm{T})^2\right)\sin\theta_{n-1}\right)^{-1}-\cot\theta_{n-1}\right)}+u_d, \end{cases} \quad (8)$$

where u_v, u_θ and u_d are the process noises with zero mean and their variances are σ_v^2, σ_θ^2 and σ_d^2, respectively[2]. The considered kinematic model given by (8) is generalized where vehicles drive at non-linear time-varying speeds.

It has been confirmed in [31] that the THz network with leaky-wave antennas is noise-limited and co-channel interference is negligible. Therefore, the sounding signal received at a vehicle is given by

$$y(t)=\sqrt{p\widetilde{G}\left(f(t),\theta(t)\right)}\hbar z(t-\tau_n)\,e^{j2\pi f_{\mathrm{Doppler}}(t)t}+\varpi_y(t). \quad (9)$$

In (9), p is the transmit power, $\widetilde{G}\left(f(t),\theta(t)\right)=\xi G\left(f(t),\theta(t)\right)$ is the effective antenna gain in which ξ can be easily obtained by measuring the effective antenna gain for a particular leaky-wave antenna structure and known a priori, $\hbar$ is the THz channel coefficient, $z(t)$ with $\mathbb{E}\{z(t)z^H(t)\}=1$ is the sounding signal, τ_n is the propagation delay, $f_{\mathrm{Doppler}}(t)$ is the Doppler shift at time t, $\varpi_y(t)$ is the complex additive white Gaussian noise with zero mean and variance σ_y^2, which is independent of the process noises in (8).

Remark 1: Different from the sensing systems with large phased arrays where multiple orthogonal narrow beams are generated to track several vehicles, the leaky-wave antenna's spatial-spectral coupling effects (signatures) enable that multiple vehicles can be identified by exploiting their unique link directions without a need for beam association. In practice, the sounding signal can be formed as a moderate "THz rainbow" [15], which only needs to consist of signal components in directions of interest (not all directions), thanks to the known prior link direction information during the tracking process.

III. Vehicle Tracking Design

In this section, we propose a new design on vehicle tracking via THz links. In contrast to the traditional phased array systems where the Doppler effect needs to be stringently evaluated in order to offer a better estimate of the propagation angle (namely sensitive to the Doppler effect), the spatial-spectral coupling feature of the leaky-wave antenna provides us a better tracking design without requiring the Doppler shift information. Specifically, based on (9), we observe the received signal strength (RSS) as

$$\overline{y}_n=p\widetilde{G}\left(f_n,\theta_n\right)|\hbar|^2+\overline{\varpi}_y, \quad (10)$$

where $\overline{\varpi}_y\sim\exp(\lambda)$ is the exponential random variable with the parameter $\lambda=1/\sigma_y^2$. Without loss of generality, we replace $\overline{\varpi}_y$ with $\widetilde{\varpi}_y=\overline{\varpi}_y-\sigma_y^2$ for facilitating the derivations such that zero mean is kept. In addition, it is noted that the channel power gain $|\hbar|^2$ can be extracted from the RSS of a pilot signal sent by the RSU at the beginning of each coherence time. To improve the accuracy of the distance measurement, the propagation delay is also observed as

$$\tau_n=\frac{d_n}{c}+\varpi_\tau, \quad (11)$$

where c is the speed of light, ϖ_τ is the noise perturbation with zero mean and its variance σ_τ^2. Thus the observation model can be written as

$$\boldsymbol{\Xi}_n=\boldsymbol{\varphi}\left(\mathbf{S}_n\right)+\boldsymbol{\varpi}_n, \quad (12)$$

where $\boldsymbol{\Xi}_n=[\overline{y}_n,\tau_n]^T$ is the observation vector, $\boldsymbol{\varphi}(\cdot)$ is the mapping function defined by (10) and (11), $\mathbf{S}_n=[v_n,\theta_n,d_n]^T$ is the state vector and $\boldsymbol{\varpi}_n=[\overline{\varpi}_y,\varpi_\tau]^T$ are the noise vector. Likewise, the state evolution model is

$$\mathbf{S}_n=\boldsymbol{\psi}\left(\mathbf{S}_{n-1}\right)+\mathbf{u}_n, \quad (13)$$

where $\boldsymbol{\psi}(\cdot)$ is defined by (8) and $\mathbf{u}_n=[u_v,u_\theta,u_d]^T$.

As indicated from (12) and (13), both the state evolution model and the observation model are real-valued and highly non-linear. Although the EKF and UKF have the same order of computational complexity [36], the UKF can overcome the approximation issues of the EKF in the non-linear systems. Therefore, we propose an UKF-based approach to estimate the states in a recursive manner, which is concluded as follows:

1) Initialization: The initial estimate of the propagation angle $\hat{\theta}_\circ$ can be obtained by using the detection scheme with a leaky-wave antenna in [23] where training is not required. Since the use of very large THz bandwidths enables highly accurate observation of the propagation delay[3], the

[1]In the realistic networks, the time scale of THz transmissions is much shorter than the vehicle dynamics. As illustrated in [40], 4.50 m/s^2 and -8.41 m/s^2 are the typical maximum acceleration and maximum deceleration that can be reached by a common modern vehicle, respectively. In the simulations, we consider the time interval $\Delta\mathrm{T}=20$ms, and the variation of speed (maximum $4.50\times0.02=0.09$m/s or $-8.41\times0.02=-0.1682$m/s) in such a time interval is tiny. Therefore, in the THz systems, it is reasonable to piecewise approximate the distribution function of the vehicle's acceleration/deceleration by partitioning it into many segments and the acceleration/deceleration value is constant in a segment's time duration.

[2]Note that these process noises have been assumed to follow Gaussian distributions in some works such as [9, 26, 27].

[3]The evaluation of propagation delay can be achieved in the initial access or synchronization phase via synchronization or reference signals.

$$\mathbf{C}_{\hat{\boldsymbol{\Xi}}_{n|n-1}} = w_0 \left(\varphi\left(\boldsymbol{\chi}_{0,n|n-1}\right) - \hat{\boldsymbol{\Xi}}_{n|n-1}\right)\left(\varphi\left(\boldsymbol{\chi}_{0,n|n-1}\right) - \hat{\boldsymbol{\Xi}}_{n|n-1}\right)^T + \sum_{i=1}^{2N} \frac{\left(\varphi\left(\boldsymbol{\chi}_{i,n|n-1}\right) - \hat{\boldsymbol{\Xi}}_{n|n-1}\right)\left(\varphi\left(\boldsymbol{\chi}_{i,n|n-1}\right) - \hat{\boldsymbol{\Xi}}_{n|n-1}\right)^T}{2\left(N+\varrho\right)} + \boldsymbol{\Lambda}_{\boldsymbol{\varpi}}, \tag{18}$$

$$\mathbf{C}_{\hat{\mathbf{S}}_{n|n-1},\hat{\boldsymbol{\Xi}}_{n|n-1}} = w_0 \left(\boldsymbol{\chi}_{0,n|n-1} - \hat{\mathbf{S}}_{n|n-1}\right)\left(\varphi\left(\boldsymbol{\chi}_{0,n|n-1}\right) - \hat{\boldsymbol{\Xi}}_{n|n-1}\right)^T + \sum_{i=1}^{2N} \frac{\left(\boldsymbol{\chi}_{i,n|n-1} - \hat{\mathbf{S}}_{n|n-1}\right)\left(\varphi\left(\boldsymbol{\chi}_{i,n|n-1}\right) - \hat{\boldsymbol{\Xi}}_{n|n-1}\right)^T}{2\left(N+\varrho\right)}, \tag{19}$$

communication distance is initialized as $\hat{d}_\circ = c\tau_\circ$ according to (11). The initial speed value $\hat{v}_\circ$ can be measured by the vehicle's odometer and the acceleration/deceleration value can be set as an arbitrary constant. Therefore, the initial state vector is $\hat{\mathbf{S}}_\circ = \mathbb{E}\{\mathbf{S}_\circ\} = \left[\hat{v}_\circ, \hat{\theta}_\circ, \hat{d}_\circ\right]^T$ and its covariance $\mathbf{C}_{\hat{\mathbf{S}}_\circ} = \boldsymbol{\Lambda}_{\mathbf{u}} = \mathrm{diag}\left(\left[\sigma_v^2, \sigma_\theta^2, \sigma_d^2\right]^T\right)$ ($\boldsymbol{\Lambda}_{\mathbf{u}}$ is the covariance of the process noise vector).

2) Statistics evaluation based on unscented transformation (UT): Unlike the EKF that needs linearized transformation via Taylor series, the UKF utilizes the UT method to directly estimate the statistics of a random variable in the non-linear systems. Specifically, let N denote the dimension of the state vector $\mathbf{S}_n$ (namely $N = 3$ in this paper), $2N+1$ symmetric sigma vectors around $\hat{\mathbf{S}}_{n-1}$ are chosen as follows:

$$\boldsymbol{\chi}_i = \begin{cases} \hat{\mathbf{S}}_{n-1},\ i = 0, \\ \hat{\mathbf{S}}_{n-1} + \sqrt{N+\varrho}\mathbf{L}_{n-1}\left(:, i\right),\ i = 1, \cdots, N, \\ \hat{\mathbf{S}}_{n-1} - \sqrt{N+\varrho}\mathbf{L}_{n-1}\left(:, i-N\right),\ i = N+1, \cdots, 2N, \end{cases} \tag{14}$$

where $\varrho = \epsilon^2\left(N+\varsigma\right) - N$, here ϵ is a small positive value [36] and ς is usually set to $3-N$ [35], $\mathbf{L}_{n-1}\left(:, m\right)$ is the m-th column of $\mathbf{L}_{n-1}$ with $\mathbf{L}_{n-1}\mathbf{L}_{n-1}^T = \mathbf{C}_{\hat{\mathbf{S}}_{n-1}}$. According to UT, the state vector is predicted to be a weighted combination of these sigma vectors, which is given by

$$\hat{\mathbf{S}}_{n|n-1} = \frac{\varrho}{N+\varrho}\boldsymbol{\chi}_{0,n|n-1} + \sum_{i=1}^{2N} \frac{\boldsymbol{\chi}_{i,n|n-1}}{2\left(N+\varrho\right)}, \tag{15}$$

where $\boldsymbol{\chi}_{0,n|n-1} = \psi\left(\boldsymbol{\chi}_0\right)$, $\boldsymbol{\chi}_{i,n|n-1} = \psi\left(\boldsymbol{\chi}_i\right)$. The covariance of $\hat{\mathbf{S}}_{n|n-1}$ is calculated as

$$\mathbf{C}_{\hat{\mathbf{S}}_{n|n-1}} = w_0 \left(\boldsymbol{\chi}_{0,n|n-1} - \hat{\mathbf{S}}_{n|n-1}\right)\left(\boldsymbol{\chi}_{0,n|n-1} - \hat{\mathbf{S}}_{n|n-1}\right)^T + \sum_{i=1}^{2N} \frac{\left(\boldsymbol{\chi}_{i,n|n-1} - \hat{\mathbf{S}}_{n|n-1}\right)\left(\boldsymbol{\chi}_{i,n|n-1} - \hat{\mathbf{S}}_{n|n-1}\right)^T}{2\left(N+\varrho\right)} + \boldsymbol{\Lambda}_{\mathbf{u}}, \tag{16}$$

where $w_o = \frac{\varrho}{N+\varrho} + \left(1 - \epsilon^2 + \vartheta\right)$ with the commonly-seen $\vartheta = 2$. Similarly, the corresponding predicted observation vector is given by

$$\hat{\boldsymbol{\Xi}}_{n|n-1} = \frac{\varrho}{N+\varrho}\varphi\left(\boldsymbol{\chi}_{0,n|n-1}\right) + \sum_{i=1}^{2N} \frac{\varphi\left(\boldsymbol{\chi}_{i,n|n-1}\right)}{2\left(N+\varrho\right)}, \tag{17}$$

and its covariance is calculated as (18) (at the top of this page), in which $\boldsymbol{\Lambda}_{\boldsymbol{\varpi}} = \mathrm{diag}\left(\left[\sigma_y^4, \sigma_\tau^2\right]^T\right)$. The cross-covariance of $\hat{\mathbf{S}}_{n|n-1}$ and $\hat{\boldsymbol{\Xi}}_{n|n-1}$ is given by (19).

3) Kalman filter gain:

$$\mathcal{K}_n = \mathbf{C}_{\hat{\mathbf{S}}_{n|n-1},\hat{\boldsymbol{\Xi}}_{n|n-1}}\mathbf{C}_{\hat{\boldsymbol{\Xi}}_{n|n-1}}^{-1}. \tag{20}$$

4) State estimation:

$$\hat{\mathbf{S}}_n = \hat{\mathbf{S}}_{n|n-1} + \mathcal{K}_n\left(\boldsymbol{\Xi}_n - \hat{\boldsymbol{\Xi}}_{n|n-1}\right). \tag{21}$$

5) State covariance:

$$\mathbf{C}_{\hat{\mathbf{S}}_n} = \mathbf{C}_{\hat{\mathbf{S}}_{n|n-1}} - \mathcal{K}_n\mathbf{C}_{\hat{\boldsymbol{\Xi}}_{n|n-1}}\mathcal{K}_n^T. \tag{22}$$

Remark 2: It is obviously seen that the proposed vehicle tracking design with leaky-wave antenna is derivative-free. The size of the real covariance matrix for the predicted observed variables (only 2×2 in this design) is less than the traditional methods with large phased arrays in which Doppler shift is an important factor and may need to be precisely measured in practice. Therefore, the inverse of the real covariance matrix for Kalman filter gain calculation given by (20) can be computed with a much lower level of complexity.

IV. Multi-vehicle Transmission Design

In the previous section, each vehicle tracks its state information by using the proposed solution and reports them to the RSU. To improve the V2I transmissions, we seek to answer how to optimize the radio resources at the RSU after receiving the state information via vehicle tracking in Section III. In particular, we highlight that user fairness concern also needs to be addressed in the considered networks, such that the quality of service (QoS) difference between vehicles is not significant and can be flexibly controlled under the rapid fluctuations of the THz V2I channels.

In the V2I networks with leaky-wave antennas, RSUs also need to know the inter-vehicle distance. The reasons are twofold: 1) minimum inter-vehicle distance in a lane should be

guaranteed to avoid collision, particularly in the ITS systems with CACC [5]; and 2) the spatial-spectral coupling feature of the leaky-wave antenna requires appropriate inter-vehicle distance to avoid the co-channel interference among vehicles, as indicated from (2). Assuming that there are K vehicles in a lane and they are served by the same RSU, based on the vehicles' feedback, the inter-vehicle distance between the vehicle $k-1$ and its predecessor vehicle k at a channel coherence time can be obtained as

$$D_{k,k-1} = \hat{d}^{k-1}\cos\hat{\theta}^{k-1} - \hat{d}^{k}\cos\hat{\theta}^{k}, \tag{23}$$

where $\hat{d}^{k-1}$ and $\hat{d}^{k}$ are the vehicles $k-1$ and k 's estimated communication distances, respectively, $\hat{\theta}^{k-1}$ and $\hat{\theta}^{k}$ are the corresponding estimated propagation angles. Substituting (2) into (23), (23) can be rewritten as

$$D_{k,k-1} = \hat{d}^{k-1}\frac{\beta\left(f^{\max}\left(\hat{\theta}^{k-1}\right)\right)}{k_0\left(f^{\max}\left(\hat{\theta}^{k-1}\right)\right)} - \hat{d}^{k}\frac{\beta\left(f^{\max}\left(\hat{\theta}^{k}\right)\right)}{k_0\left(f^{\max}\left(\hat{\theta}^{k}\right)\right)}. \tag{24}$$

It is explicitly shown from (24) that varying inter-vehicle distances have an effect on the frequency allocation.

The transmission rate of the vehicle k is given by

$$R_k = \sum_{\xi} m_{k,\xi} B_{k,\xi}\log_2\left(1+\frac{\gamma_{k,\xi}\left(f_{k,\xi}\right)}{\bar{\sigma}^2}\right), \tag{25}$$

where $m_{k,\xi}$ is the binary indicator, $B_{k,\xi}$ is the vehicle k's ξ-th strongest subchannel[4] bandwidth with the carrier frequency $f_{k,\xi}$, $\gamma_{k,\xi}\left(f_{k,\xi}\right) = q_{k,\xi}\widetilde{G}\left(f_{k,\xi},\theta_k\right)\left|\hbar_{k,\xi}\right|^2$ is the receive power spectral density (PSD) with the transmit PSD $q_{k,\xi}$, and $\bar{\sigma}^2$ is the PSD of the noise. Our aim is to maximize the sum rate under the user fairness concern in such a dynamic environment, the considered problem is formulated as

$$\begin{aligned}
&\max_{\mathbf{m},\mathbf{B},\mathbf{f},\mathbf{q}} \sum_{k=1}^{K} R_k \qquad (26)\\
&\text{s.t. C1}: m_{k,\xi}\in\{0,1\}, \quad \forall k,\forall\xi,\\
&\text{C2}: \sum_{k=1}^{K} m_{k,\xi} = 1, \quad \forall\xi,\\
&\text{C3}: \frac{\gamma_{k,\xi}\left(f_{k,\xi}\right)}{\bar{\sigma}^2} \geq \bar{\gamma}_{\text{th}}, \quad \forall k,\forall\xi,\\
&\text{C4}: \frac{R_k}{R_{k'}} = \frac{r_k}{r_{k'}}, \quad \forall k\in\{1,\cdots,K\},\forall k'\in\{1,\cdots,K\},\\
&\text{C5}: \sum_{k=1}^{K}\sum_{\xi} m_{k,\xi}B_{k,\xi} \leq B_{\text{total}},\\
&\text{C6}: \bigcap_{k,\xi}\left\{f \,\middle|\, f\in\left[f_{k,\xi}-\frac{B_{k,\xi}}{2}, f_{k,\xi}+\frac{B_{k,\xi}}{2}\right]\right\} = \emptyset,\\
&\text{C7}: \left\|\gamma_{k,\xi}\left(f_{k,\xi}-\frac{B_{k,\xi}}{2}\right)|_{\text{dB}} - \gamma_{k,\xi}\left(f_{k,\xi}+\frac{B_{k,\xi}}{2}\right)|_{\text{dB}}\right\| \leq \varepsilon,\\
&\text{C8}: D_{k,k-1} \geq D_{\text{safety}}, \quad \forall k,\\
&\text{C9}: \sum_{k=1}^{K}\sum_{\xi} m_{k,\xi}B_{k,\xi}q_{k,\xi} \leq q_{\text{total}},\\
&\text{C10}: B_{k,\xi}\geq 0, \quad q_{k,\xi}\geq 0, \quad \forall k,\forall\xi,
\end{aligned}$$

where $\mathbf{m}=[m_{k,\xi}]$, $\mathbf{B}=[B_{k,\xi}]$, $\mathbf{f}=[f_{k,\xi}]$, $\mathbf{q}=[q_{k,\xi}]$. Constraints C1 and C2 guarantee that each subchannel is solely allocated, in order to avoid the co-channel interference between vehicles; C3 ensures that the minimum QoS is met with the threshold $\bar{\gamma}_{\text{th}}$; C4 describes the rate fairness concern with the pre-set values $\{r_k\}_{k=1}^{K}$, thus the expected Jain's fairness index is $\left(\sum_{k=1}^{K} r_k\right)^2 / \left(K\sum_{k=1}^{K} r_k^2\right)$ and the perceived fairness expected by the vehicle k is $\bar{\Theta}_k = r_k \sum_{k=1}^{K} r_k / \sum_{k=1}^{K} r_k^2$ [41]; C5 illustrates the total available bandwidth B_{total}; C6 and C7 define the THz subchannel, namely no overlap between subchannels and the RSS difference below a small value ε in the frequencies of a subchannel; C8 indicates the spatial-spectral coupling effect given a safe distance D_{safety} in light of (24); C9 is the power consumption limitation; C10 ensures that $B_{k,\xi}$ and $q_{k,\xi}$ are non-negative values.

Problem (26) is combinatorial and the feasible set is non-convex, which is challenging to solve in the THz V2I communications with much lower latency. Therefore, we develop an efficient suboptimal algorithm with low-complexity. To this end, we first study the subproblem involving subchannel allocation based on (26), which is as follows:

$$\begin{aligned}
&\max_{\mathbf{m},\mathbf{B},\mathbf{f}} \sum_{k=1}^{K} R_k \qquad (27)\\
&\text{s.t. C1, C2, C3, C4, C5, C6, C7, C8,}\\
&\quad B_{k,\xi}\geq 0, \quad \forall k,\forall\xi.
\end{aligned}$$

The optimal solution of problem (27) is hard to find, due to the fact that the antenna gain of the leaky-wave antenna cannot be explicitly computed. We realize that each vehicle leverages at least one subchannel for information transmissions in practice, namely $m_{k,1}=1,\forall k$. Therefore, with the help of algorithm 1 in [31] [5], we can first obtain each vehicle's strongest subchannel $\{B_{k,1}^{*}, f_{k,1}^{*}\}$ based on the estimated propagation angle and the channel power gain at the initial stage. Then, the transmission rate R_k of each vehicle is calculated and the vehicle k's perceived fairness is calculated as [41]

$$\Theta_k = R_k \sum_{k=1}^{K} R_k / \sum_{k=1}^{K} R_k^2. \tag{28}$$

To satisfy the user fairness constraint C4, the most discriminated vehicle with the minimum value of $\{\Theta_k - \bar{\Theta}_k\}$ is chosen to add a new subchannel based on algorithm 1 in [31]. Moreover, the newly added subchannel's frequencies also have to meet the constraint C8 in light of safe driving and co-channel interference avoidance, i.e., the value of the guard band between a vehicle and its neighboring vehicle should

[4]Here, a strong subchannel means that given the same transmit power, high spectral efficiency can be achieved by using such a subchannel.

[5]In [31], subchannel allocation for rate maximization under the constraints C3 and C5-C7 has been addressed in the point-to-point system with a leaky-wave antenna.

always be non-negative, which can be measured by

$$B_{k-1,1:\xi_{\_}} + B_{k,1:\xi^{-}} \leq \frac{f_{\mathrm{co}}}{\sin\hat{\theta}^{k-1}} - \frac{\hat{d}^{k} f_{\mathrm{co}}}{\sqrt{\left(\hat{d}^{k}\right)^{2} - \left(\hat{d}^{k-1}\cos\hat{\theta}^{k-1} - D_{\mathrm{safety}}\right)^{2}}} \tag{29}$$

where $B_{k-1,1:\xi_{\_}}$ is part of the vehicle $k-1$'s frequency band below $f^{\max}\left(\hat{\theta}^{k-1}\right)$, $\xi_{\_}$ denotes the number of subchannels below $f^{\max}\left(\hat{\theta}^{k-1}\right)$, and $B_{k,1:\xi^{-}}$ is part of the vehicle k's frequency band above $f^{\max}\left(\hat{\theta}^{k}\right)$ ($f^{\max}\left(\hat{\theta}^{k-1}\right) > f^{\max}\left(\hat{\theta}^{k}\right)$), ξ^{-} denotes the number of subchannels above $f^{\max}\left(\hat{\theta}^{k}\right)$, $B_{k-1,1:\xi_{\_}}$ and $B_{k,1:\xi^{-}}$ are calculated as

$$B_{k-1,1:\xi_{\_}} = \frac{B^{*}_{k-1,1}}{2} + f^{\max}\left(\hat{\theta}^{k-1}\right) - f^{*}_{k-1,1} + \sum_{\xi=2}^{\xi_{\_}} B^{*}_{k-1,\xi}, \tag{30}$$

$$B_{k,1:\xi^{-}} = \frac{B^{*}_{k,1}}{2} + f^{*}_{k,1} - f^{\max}\left(\hat{\theta}^{k}\right) + \sum_{\xi=2}^{\xi^{-}} B^{*}_{k,\xi}. \tag{31}$$

The selected subchannel that satisfies (29) is added by the most discriminated vehicle, then it updates its transmission rate given by (25) and perceived fairness value given by (28). As such, the subchannels is iteratively allocated until the Jain's fairness index is unchanged (each vehicle's perceived fairness is stable), which is summarized as follows:

Stage 1: Given the equal power allocation, each vehicle's strongest subchannel $\{B^{*}_{k,1}, f^{*}_{k,1}\}$ ($m_{k,1} = 1, k = 1, \cdots, K$) is determined by using the algorithm 1 in [31], and each vehicle's transmission rate and perceived fairness given by (28) are calculated accordingly.

Stage 2: Repeat

a) Select the most discriminated vehicle that has the minimum value of $\{\Theta_k - \bar{\Theta}_k\}$. Then, the selected vehicle adds a new subchannel based on the algorithm 1 in [31], which also needs to meet the condition (29), otherwise there is no additional subchannel that can be allocated to the selected vehicle and it will be excluded from subchannel allocation in the following iterations;

b) Update the selected vehicle's transmission rate and perceived fairness.

Until convergence (Jain's fairness index becomes stable), and obtain the corresponding subchannel allocation $\{m^{*}_{k,\xi}, B^{*}_{k,\xi}, f^{*}_{k,\xi}\}$.

After fixing the subchannels based on the proposed method, we proceed to study the subproblem involving power allocation based on (26), i.e.,

$$\begin{aligned} &\max_{\mathbf{q}} \sum_{k=1}^{K} R_k \\ &\text{s.t. C3, C9,} \\ &\quad \mathrm{C4}: r_1 R_k - r_k R_1 = 0, \quad \forall k = 2, \cdots, K, \\ &\quad q_{k,\xi} \geq 0, \quad \forall k, \forall \xi. \end{aligned} \tag{32}$$

The problem (35) can be referred to as the maximization for the weighted sum of spectral efficiency mentioned in [42, 43]. However, the issue is that the user fairness constraint C4 has the difference of convex form. To quickly tackle this issue, we adopt the convex-concave procedure, which transforms C4 as

$$r_1 R_k - r_k R_1|_{q_{1,\xi}=q^{pr}_{1,\xi}} - r_k \sum_{\xi} \frac{\partial R_1}{\partial q_{1,\xi}}|_{q_{1,\xi}=q^{pr}_{1,\xi}} \left(q_{1,\xi} - q^{pr}_{1,\xi}\right) \geq 0, \tag{33}$$

and

$$r_k R_1 - r_1 R_k|_{q_{k,\xi}=q^{pr}_{k,\xi}} - r_1 \sum_{\xi} \frac{\partial R_k}{\partial q_{k,\xi}}|_{q_{k,\xi}=q^{pr}_{k,\xi}} \left(q_{k,\xi} - q^{pr}_{k,\xi}\right) \geq 0, \tag{34}$$

where $q^{pr}_{1,\xi}$ is the optimal value at the last iteration. As such, we solve the problem (35) in an iterative manner, i.e., in each iteration, we address the problem as follows:

$$\begin{aligned} &\max_{\mathbf{q}} \sum_{k=1}^{K} R_k \\ &\text{s.t. C3, C9,} \\ &\quad \tilde{\mathrm{C}}4: (33), (34), \quad \forall k = 2, \cdots, K, \\ &\quad q_{k,\xi} \geq 0, \quad \forall k, \forall \xi. \end{aligned} \tag{35}$$

Problem (35) is convex and can be efficiently solved by CVX [44].

Remark 3: Given the rapid fluctuation and ultra-low coherence time of the THz V2I channel, we focus on a low-complexity approach to address the problem (26). Specifically, the optimal subchannel allocation $\{m^{*}_{k,\xi}, B^{*}_{k,\xi}, f^{*}_{k,\xi}\}$ is determined by solving (27) under the equal power allocation. Based on $\{m^{*}_{k,\xi}, B^{*}_{k,\xi}, f^{*}_{k,\xi}\}$, the corresponding power allocation $\{q^{*}_{k,\xi}\}$ is obtained by solving (35). As such, we obtain the desired solution $\{m^{*}_{k,\xi}, B^{*}_{k,\xi}, f^{*}_{k,\xi}, q^{*}_{k,\xi}\}$ of the problem (26). Another benefit of the proposed design is that it is easy to tune the subchannel number of each vehicle for meeting the peak-to-average power ratio constraint [45].

The convergence of the proposed resource allocation solution is guaranteed since the subchannel allocation is based on the vehicle's perceived fairness order with a complexity ordered by $\mathcal{O}(N)$ and the power allocation corresponds to the transformed convex problem that can be efficiently solved by CVX, hence the proposed solution provides an acceptable complexity.

V. Simulation Results

This section provides numerical results to confirm the efficiency of the proposed tracking design in Section III and information transmission design with user fairness awareness in Section IV. In the simulations, the leaky-wave antenna's parameters include the aperture length $\ell = 0.045$m and the inter-plate distance $L = 3.5$mm. The observation time interval $\Delta\mathrm{T} = 20$ms. The vehicle's acceleration remains constant within one observation time interval and changes following the Gaussian distribution with the mean a_{E} and the variance 9×10^{-4} (namely $a \sim \mathcal{N}\left(a_{\mathrm{E}}, 9 \times 10^{-4}\right)$) in the next observation time. The free-space path loss (FSPL)

model is utilized since it can well predict the channel of LoS THz link for low range transmissions [10, 46]. The variances of the process noises in the state evolution model (8) are $\sigma_v^2 = 1 \times 10^{-2}$, $\sigma_\theta^2 = 4 \times 10^{-4}$ and $\sigma_d^2 = 2.5 \times 10^{-3}$, respectively, and the variances of the noises in the observation model are $\sigma_y^2 = 9 \times 10^{-2}$ and $\sigma_\tau^2 = 4 \times 10^{-20}$, respectively. The other simulation parameters are detailed in the following simulation results.

A. Performance of the Proposed Tracking Solution

In the simulations, the transmit power is $p = 30$dBm, the leaky-wave antenna's attenuation coefficient is $\alpha = 90$rad/m, the minimum communication distance between a vehicle and the RSU is $h = 5$m. Without loss of generality, we provide an example of tracking one vehicle. The initial states of the considered vehicle include the velocity $v_\circ = 20$m/s, the direction $\theta_\circ = 5^\circ$ and thus the initial communication distance $d_\circ = h/\sin\theta_\circ = 57.36$m.

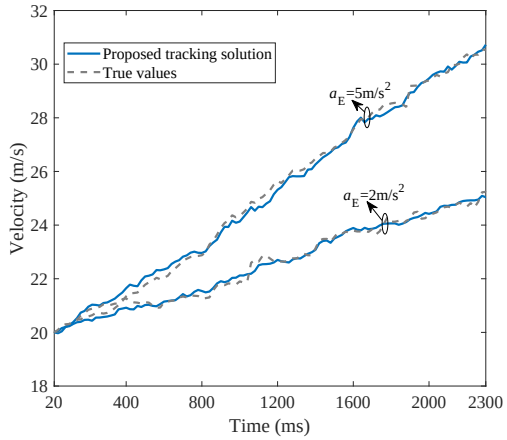

Fig. 2. Velocity estimates versus true values.

Fig. 2 shows the velocity estimates for different mean values of the acceleration. The proposed tracking solution can keep an accurate estimation of the vehicle's driving speed during the acceleration phase, and different levels of acceleration have minimal effect on the velocity tracking. One big reason is that the proposed tracking solution with the leaky-wave antenna is non-coherent and the Doppler effects caused by high mobility can be mitigated.

Fig. 3 shows the propagation angle estimates for different mean values of the acceleration. The proposed tracking solution can estimate the propagation angle with high accuracy. Although the propagation angle changes fast at high speed, its effect on the tracking performance is limited. We see that the proposed tracking solution performs well for different levels of acceleration. The reason is that the leaky-wave antenna's spatial-spectral coupling feature enables that the angle can be well identified by only measuring the RSS.

Fig. 4 shows the V2I communication distance estimates for different mean values of the acceleration. Based on our tracking design, the V2I communication distance is well evaluated. Again, we see that different levels of acceleration

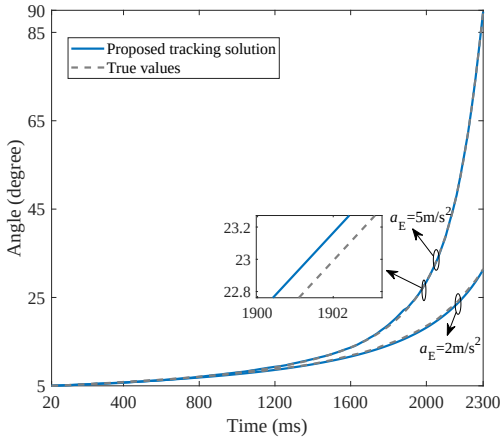

Fig. 3. Propagation angle estimates versus true values.

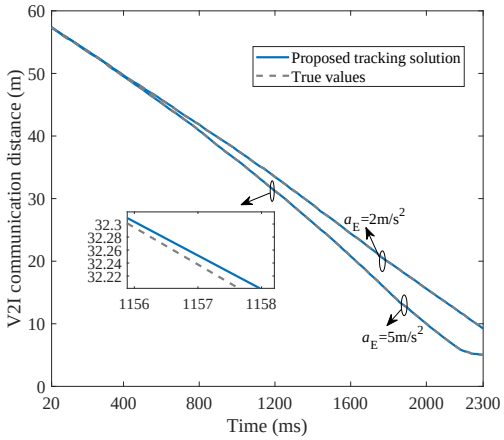

Fig. 4. V2I communication distance estimates versus true values.

have negligible effects on the communication distance tracking performance, thanks to our non-coherent tracking design with THz transmission in a nano-second time scale.

B. Comparisons with Cramer-Rao Lower Bound (CRLB)

In this subsection, we investigate the performance behaviors of the proposed tracking solution and Cramer-Rao lower bound (CRLB) in terms of the root mean square error (RMSE), to further demonstrate the efficiency of our tracking design. It is known that CRLB is the lower bound on the mean square error (MSE) of any unbiased estimator and can be easily obtained by following the approach mentioned in [34, Appendix 3B]. In the simulations, the root of the CRLB is the benchmark, the acceleration's mean is assumed to be $a_{\rm E} = 5$m/s^2 and other basic simulation parameters are the same as those mentioned in subsection V-A.

Fig. 5(a) shows the RMSE of the estimated velocity achieved by the proposed tracking solution and the CRLB. We first see that slightly increasing the leaky-wave antenna's attenuation coefficient can reduce the estimation error. The reason is that the receive signal power is enhanced and thus the adverse effect of the noise in the RSS observation becomes less

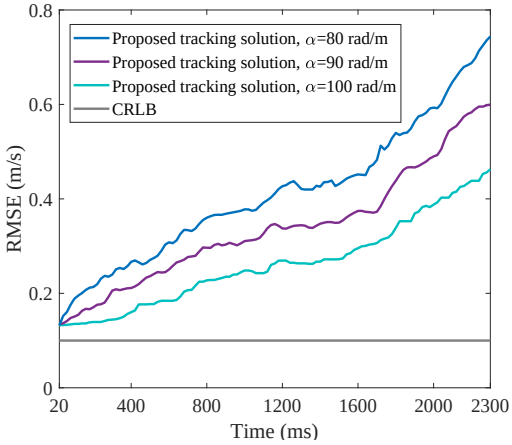

(a) Proposed tracking solution

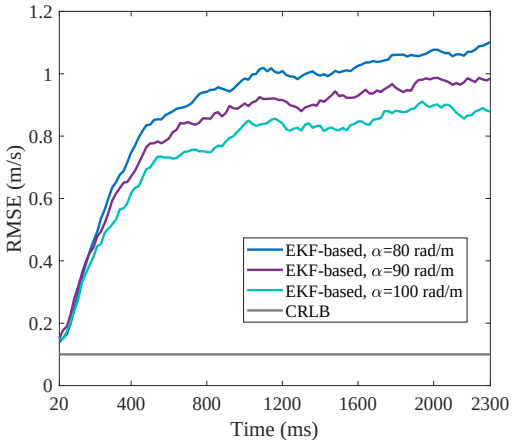

(b) EKF-based solution

Fig. 5. The root mean square error (RMSE) for estimating the velocity.

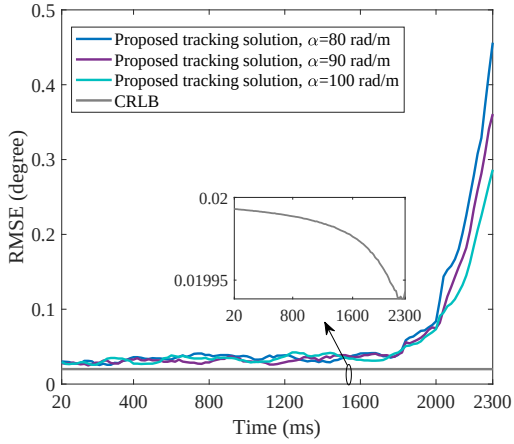

(a) Proposed tracking solution

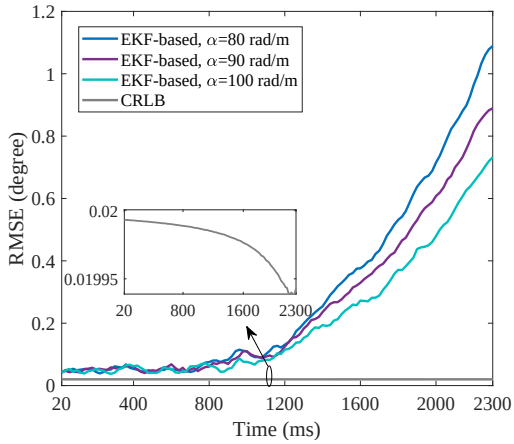

(b) EKF-based solution

Fig. 6. The root mean square error (RMSE) for estimating the propagation angle.

severe. Although the CRLB gives the lowest level of RMSE in this case, the proposed tracking solution still performs a much lower level of RMSE when noting that the vehicle's initial velocity is $v_\circ = 20$m/s and its velocity can be above $v_\circ = 30$m/s after acceleration as seen in Fig. 2. The performance gap between the proposed tracking solution and the CRLB increases over the time. This is because that the proposed tracking design relies on the prior state information, but the vehicle's states change much faster between two consecutive observations when its velocity is higher, which makes the state and observation predictions less accurate based on the prior state information. To improve the estimation accuracy in the scenario with significantly high mobility, increasing tracking frequency (shorter observation time interval) may be required, however, the tradeoff between tracking frequency and system overhead needs to be balanced in practice. The proposed tracking solution substantially outperforms the EKF-based counterpart shown in Fig. 5(b) since the system is highly non-linear.

Fig. 6(a) shows the RMSE of the estimated propagation angle achieved by the proposed tracking solution and the CRLB. By exploiting the leaky-wave antenna's spatial-spectral coupling effects, the performance of our tracking design is close to the CRLB when the vehicle's velocity is below a critical value. Another reason is that the Doppler effect caused by mobility is irrelevant to the estimation in our tracking solution since the Doppler shift observation is unnecessary. The estimation error decreases when slightly increasing the leaky-wave antenna's attenuation coefficient because of the stronger received signal power. As mentioned before, higher mobility leads to the rapid variations of the vehicle's states, which deteriorate the state and observation predictions. It is shown in Fig. 6(b) that the EKF-based solution is much more sensitive to the high mobility and has larger RMSE than our tracking solution.

Fig. 7(a) shows the RMSE of the estimated V2I communication distance achieved by the proposed tracking solution and the CRLB. The performance gap between the proposed tracking solution and the CRLB is marginal. Again, we see that slightly increasing the leaky-wave antenna's attenuation coefficient improves the estimation accuracy. As seen in Fig. 7(b), the EKF-based solution has less estimation accuracy compared with the proposed tracking solution.

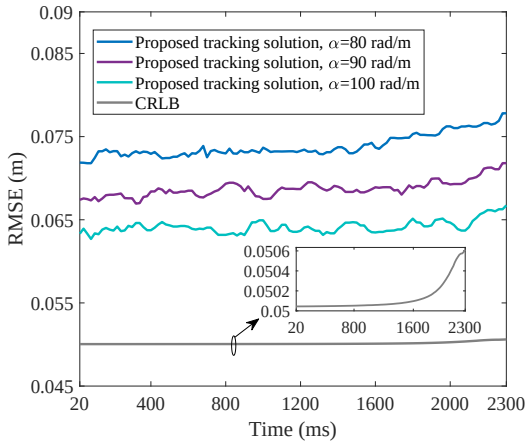

(a) Proposed tracking solution

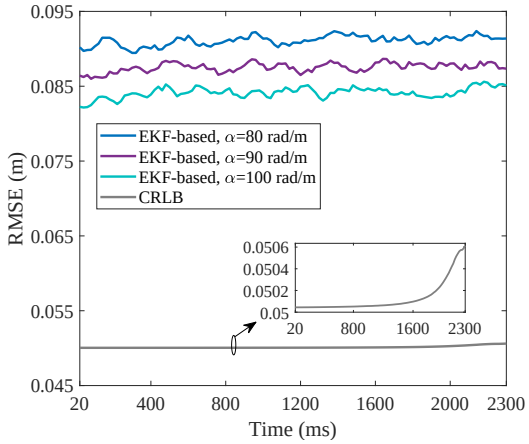

(b) EKF-based solution

Fig. 7. The root mean square error (RMSE) for estimating the V2I communication distance.

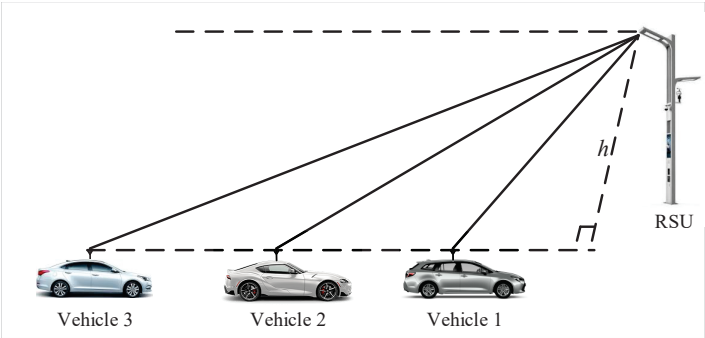

Fig. 8. An illustration of three vehicles connected to the RSU.

C. Transmission Design with User Fairness Awareness

In this subsection, we investigate the performance of the proposed transmission design with user fairness awareness in the multi-vehicle scenarios. The RSS-based subchannel allocation with equal transmit PSD is considered as the baseline algorithm, where a vehicle is selected to use a subchannel if it has the highest RSS in this subchannel, and thus more subchannels are allocated to the vehicles with better channel conditions and larger antenna gains. In the simulations, we consider that the RSU is connected to three vehicles located in the same lane as shown in Fig. 8, where vehicle 1's initial states include the velocity $v_{1,\circ} = 20$m/s, the direction $\theta_{1,\circ} = 6.2°$ and the mean of its acceleration $a_{1,\mathrm{E}} = 4.5\mathrm{m/s}^2$; vehicle 2's initial states include the velocity $v_{2,\circ} = 20$m/s, the direction $\theta_{2,\circ} = 5.6°$ and the mean of its acceleration $a_{2,\mathrm{E}} = 4\mathrm{m/s}^2$; and vehicle 3's initial states include the velocity $v_{3,\circ} = 20$m/s, the direction $\theta_{3,\circ} = 5°$ and the mean of its acceleration $a_{3,\mathrm{E}} = 3.5\mathrm{m/s}^2$. The leaky-wave antenna's attenuation coefficient is $\alpha = 90$rad/m and other parameters are shown in Table I.

TABLE I
SIMULATION PARAMETERS

Equal transmit PSD	$q = -71.76$dBm/Hz
Noise's PSD	$\bar{\sigma}^2 = -174$dBm/Hz
Threshold for the minimum QoS	$\bar{\gamma}_{\mathrm{th}} = -7.5$dB
RSS gap in the frequencies of a subchannel below ε	$\varepsilon = 0.1$dB
Total transmit power	$q_{\mathrm{total}} = q * B_{\mathrm{total}}$

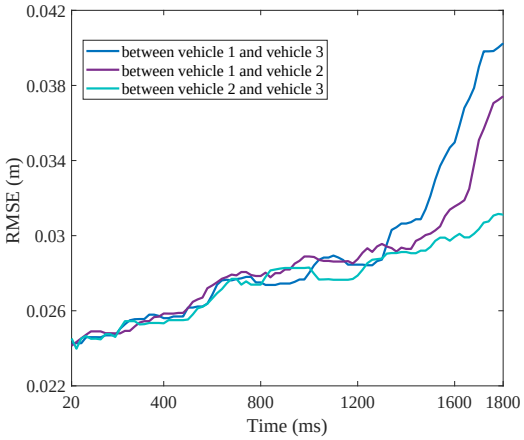

Fig. 9. The root mean square error (RMSE) for estimating the inter-vehicle distance with the transmit power $p = 30$dBm and $h = 5$m.

Fig. 9 shows the root mean square error (RMSE) for estimating the inter-vehicle distance. The inter-vehicle distance needs to be well estimated because it not only plays a key role in the ITS systems [5] but also has an impact on the frequency allocation as indicated from (24). It is seen that by using our tracking design, the estimation error is minimal and increases slowly during the acceleration phase. Since vehicle 1 and vehicle 2 move faster than vehicle 3, the error of estimating the distance between vehicle 1 and vehicle 2 is larger than that between vehicle 2 and vehicle 3, and the error is further enlarged by estimating the longer distance between vehicle 1 and vehicle 3.

Fig. 10 shows the performance for the average sum rate and Jain's fairness index versus the minimum communication distance with different expected values of the Jain's fairness index. In Fig. 10(a), we see that the proposed solution outperforms the RSS-based subchannel allocation with equal transmit PSD and the performance gap increases when the minimum communication distance grows large. The performance gap is not significant when the minimum communication distance is very small (e.g., 3m in Fig. 10), due to the fact

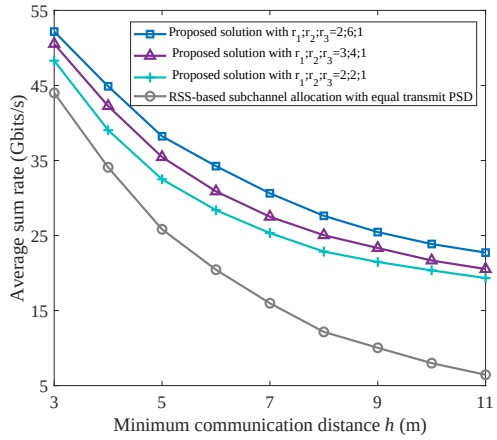

(a) Average sum rate

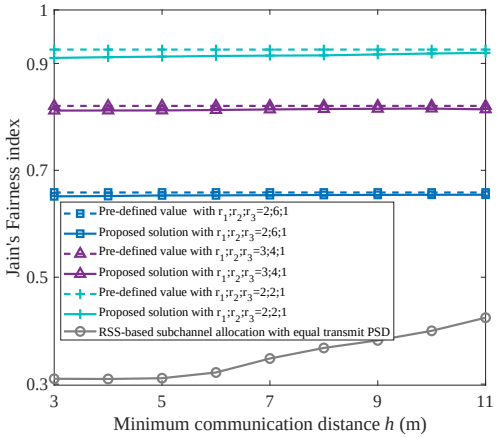

(b) Jain's fairness index

Fig. 10. The performance for average sum rate and Jain's fairness index versus the minimum communication distance with the total available bandwidth $B_{\text{total}} = 15$GHz, safe distance $D_{\text{safety}} = 5$m and other simulation parameters in Table I.

that the vehicles closest to the RSU play a dominate role in the average sum rate. Since vehicle 1 and vehicle 2 are closer to the RSU than vehicle 3 (better channel conditions), the average sum rate is improved as more subchannels and transmit power are allocated to the vehicle 1 and vehicle 2[6]. The performance gap becomes insignificant for different pre-set Jain's fairness index values when the minimum communication distance is large because there are not many available radio resources that can meet the QoS requirement; In Fig. 10(b), we see that the expected Jain's fairness index can be fulfilled by using our solution, and the baseline algorithm achieves the lowest level of Jain's fairness index since most of subchannels are allocated to the vehicles with better channel conditions. Moreover, it is shown that there is indeed a tradeoff between the average sum rate and user fairness, i.e., higher average sum rate results in the loss of user fairness[7]. An interesting phenomenon for the baseline algorithm is that Jain's fairness index is improved when increasing the minimum communication distance, due to the decreasing transmission rate gap between vehicles. Therefore, it is confirmed from Figs. 10(a) and 10(b) that the proposed solution is highly efficient and can well strike a balance between the average sum rate and user fairness for different values of the minimum communication distance.

[6]In the simulation results, larger r_k means that the k-th user requires higher transmission rate, namely more radio resources.

[7]In the simulation results, larger r_k means that the k-th user requires more radio resources, but reduces the Jain's fairness index.

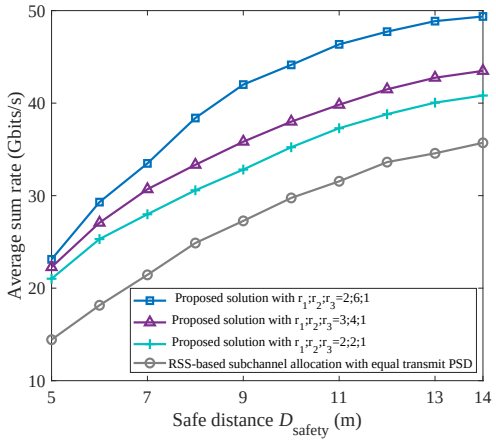

(a) Average sum rate

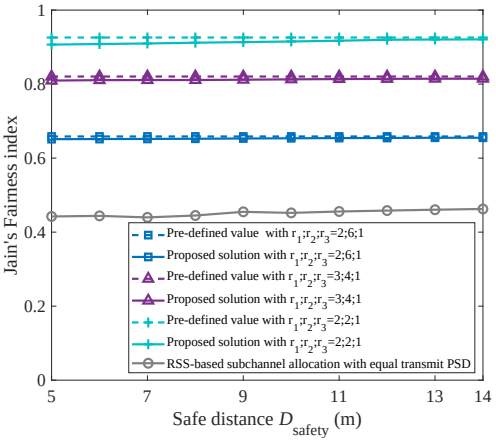

(b) Jain's fairness index

Fig. 11. The performance for average sum rate and Jain's fairness index versus the safe distance between vehicles with the total available bandwidth $B_{\text{total}} = 10$GHz, $h = 5$m and other simulation parameters in Table I.

Fig. 11 shows the performance for the average sum rate and Jain's fairness index versus the safe distance with different expected values of the Jain's fairness index. In Fig. 11(a), the proposed solution achieves higher average sum rate than the baseline algorithm. The average sum rate is enhanced when increasing the safe distance, due to the fact that more non-overlapping bandwidths between vehicles can be used as indicated in (29), which also explains that the average sum rate is greatly improved by allocating more radio resources to the vehicle 1 and vehicle 2; In Fig. 11(b), we see that by using the proposed solution, the expected Jain's fairness index is guaranteed for different safe distance values and the baseline algorithm keeps a much lower level of user fairness. Therefore, Figs. 11(a) and 11(b) demonstrate the efficiency of the proposed solution, which can well strike a balance

between the average sum rate and user fairness for different safe distance values.

Fig. 12 shows the performance for the average sum rate and Jain's fairness index versus the total available bandwidth with different expected values of the Jain's fairness index. In Fig. 12(a), it is obviously seen that the proposed solution performs better than the baseline algorithm and increasing the total available bandwidth brings in a large increase in the average sum rate. When the total available bandwidth is large enough (above 16 GHz in this figure), the average sum rate can increase more rapidly if more bandwidths are allocated to the vehicle 1 and vehicle 2 with better channel conditions (e.g., $r_1; r_2; r_3 = 2; 6; 1$ in this figure); In Fig. 12(b), the proposed solution can ensure that the expected user fairness is kept and achieves higher level of user fairness than the baseline algorithm. Lowering the rate gap can improve the user fairness, which needs to be appropriately determined in practice. It is noted that increasing the total available bandwidth significantly harms the performance of the baseline algorithm, because more bandwidths are allocated to the vehicles with better channel conditions. Therefore, Figs. 12(a) and 12(b) demonstrate the efficiency of the proposed solution, which can well strike a balance between the average sum rate and user fairness for different values of the total available bandwidth.

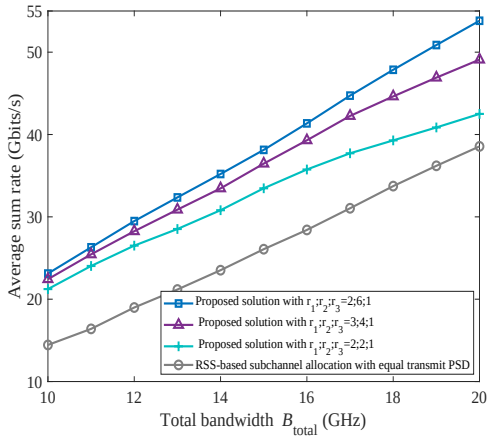

(a) Average sum rate

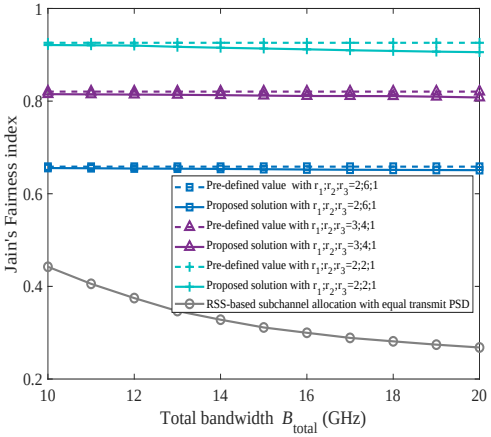

(b) Jain's fairness index

Fig. 12. The performance for average sum rate and Jain's fairness index versus the total available bandwidth with $h = 5$m, safe distance $D_{\text{safety}} = 5$m and other simulation parameters in Table I.

VI. Conclusions and Future Work

In the multi-vehicle THz V2I networks, vehicle tracking and transmission design play a key role in the intelligent V2X communications. With the assistance of the angle-frequency coupling of leaky-wave antenna, we designed an UKF-based tracking solution to estimate the vehicle's velocity, direction and communication distance. Different from the existing methods, our design did not require the measurements of the Doppler shift. The simulation results have confirmed the efficiency of the proposed tracking solution and shown that our performance with moderate tracking frequency is close to the CRLB when the vehicle's velocity is not significantly high. Then, we concentrated on addressing the issue of user fairness when allocating the radio resources in the highly dynamic THz V2I networks, which has not been investigated before. Considering the fact that the computational complexity cannot be high in the THz communications with ultra-low latency, we proposed a low-complexity approach to maximize the sum rate while guaranteeing the user fairness through proper subchannel and power allocation. The simulation results have confirmed that the proposed subchannel and power allocation method can achieve higher sum rate without the loss of the desired user fairness.

This paper has demonstrated the benefits of using leaky-wave antennas in the multi-vehicle THz V2I networks, however, more research attention needs to be paid to considering various scenarios. As mentioned before, the tracking frequency should be appropriately selected to support significantly high mobility without adding much system overhead and some adaptive approaches may also be feasible. Although the implementation of conventional phased arrays in the THz V2I systems is challenging [25], appropriate performance comparisons between the leaky-wave antenna and conventional phased arrays in such mobile scenarios need to be studied. Moreover, building the efficient multi-face leaky-wave antenna structure is an intuitive engineering work to achieve the required propagation angle coverage for a specific THz frequency bandwidth, and selecting the optimal cutoff frequency for the TE_1 mode leaky-wave antenna may also further improve the propagation angle coverage. Furthermore, the V2I-based tracking design for the ITS systems such as CACC is an important area that warrants further study.

References

[1] Z. Lin, L. Wang, J. Ding, Y. Xu and B. Tan, "V2I-aided tracking design," *IEEE Int. Conf. Commun. (ICC)*, 2022, pp. 291-296.

[2] 3GPP TS 22.185, "Service requirements for V2X services; Stage 1 (Release 16)," July 2020.

[3] V. Milanés, J. Villagrá, J. Godoy, J. Simó, J. Pérez, and E. Onieva, "An intelligent V2I-based traffic management system," *IEEE Trans. Intell. Transp. Syst.*, vol. 13, no. 1, pp. 49–58, Mar. 2012.

[4] Y.-Y. Lin and I. Rubin, "Infrastructure aided networking and traffic management for autonomous transportation," in *IEEE Inf. Theory Appl. Workshop (ITA)*, 2017, pp. 1–7.

[5] L. Wang, Y. Duan, Y. Lai, S. Mu, and X. Li, "V2I-based platooning design with delay awareness," *arXiv preprint arXiv:2012.03243*, Dec. 2020.

[6] Y. Wang, G. de Veciana, T. Shimizu, and H. Lu, "Deployment and performance of infrastructure to assist vehicular collaborative sensing," in *IEEE VTC*, 2018, pp. 1–5.

[7] H. Wymeersch, G. Seco-Granados, G. Destino, D. Dardari, and F. Tufvesson, "5G mmwave positioning for vehicular networks," *IEEE Wireless Commun.*, vol. 24, no. 6, pp. 80–86, Dec. 2017.

[8] N. Gonzalez-Prelcic, R. Mendez-Rial, and R. W. Heath, "Radar aided beam alignment in mmwave V2I communications supporting antenna diversity," *Proc. Inf. Theory Appl. Workshop (ITA)*, Jan. 2016, pp. 1–7.

[9] F. Liu, W. Yuan, C. Masouros, and J. Yuan, "Radar-assisted predictive beamforming for vehicular links: Communication served by sensing," *IEEE Trans. Wireless Commun.*, vol. 19, no. 11, pp. 7704–7719, Nov. 2020.

[10] T. S. Rappaport *et al.*, "Wireless communications and applications above 100 GHz: Opportunities and challenges for 6G and beyond," *IEEE Access*, vol. 7, pp. 78 729–78 757, June 2019.

[11] M. Polese, J. M. Jornet, T. Melodia, and M. Zorzi, "Toward end-to-end, full-stack 6G terahertz networks," *IEEE Commun. Mag.*, vol. 58, no. 11, pp. 48–54, Nov. 2020.

[12] K. Rikkinen, P. Kyöti, M. E. Leinonen, M. Berg, and A. Pärssinen, "THz radio communication: Link budget analysis toward 6G," *IEEE Commun. Mag.*, vol. 58, no. 11, pp. 22–27, Nov. 2020.

[13] H. Sarieddeen, N. Saeed, T. Y. Al-Naffouri, and M.-S. Alouini, "Next generation terahertz communications: A rendezvous of sensing, imaging, and localization," *IEEE Commun. Mag.*, vol. 58, no. 5, pp. 69–75, May 2020.

[14] X. Fu, F. Yang, C. Liu, X. Wu, and T. J. Cui, "Terahertz beam steering technologies: From phased arrays to field-programmable metasurfaces," *Adv. Opt. Mater.*, vol. 8, no. 3, pp. 1–22, Feb. 2020.

[15] Y. Ghasempour, C. Yeh, R. Shrestha, D. Mittleman, and E. Knightly, "Single shot single antenna path discovery in THz networks," in *Proc. 26th MobiCom*, 2020, pp. 1–13.

[16] D. Headland, Y. Monnai, D. Abbott, C. Fumeaux, and W. Withayachumnankul, "Tutorial: Terahertz beamforming, from concepts to realizations," *APL Photonics*, vol. 3, no. 5, pp. 1–32, 2018.

[17] I. Frigyes and A. J. Seeds, "Optically generated true-time delay in phased-array antennas," *IEEE Trans. Microw. Theory Techn.*, vol. 43, no. 9, pp. 2378–2386, Sept. 1995.

[18] D. R. Jackson and A. A. Oliner, "Leaky-wave antennas," in Modern Antenna Handbook, C. Balanis, Ed. New York: Wiley, 2008.

[19] C.-Y. Yeh, Y. Ghasempour, Y. Amarasinghe, D. M. Mittleman, and E. W. Knightly, "Security in terahertz WLANs with leaky wave antennas," in *ACM WiSec*, 2020, pp. 1–11.

[20] K. Murano, I. Watanabe, A. Kasamatsu, S. Suzuki, M. Asada, W. Withayachumnankul, T. Tanaka, and Y. Monnai, "Low-profile terahertz radar based on broadband leaky-wave beam steering," *IEEE Trans. Terahertz Sci. Technol.*, vol. 7, no. 1, pp. 60–69, Jan. 2017.

[21] H. Matsumoto, I. Watanabe, A. Kasamatsu, and Y. Monnai, "Integrated terahertz radar based on leaky-wave coherence tomography," *Nature Electronics*, vol. 3, pp. 122–129, Feb. 2020.

[22] N. J. Karl, R. W. McKinney, Y. Monnai, R. Mendis, and D. M. Mittleman, "Frequency-division multiplexing in the terahertz range using a leaky-wave antenna," *Nature Photonics*, vol. 9, pp. 717–721, Sept. 2015.

[23] Y. Ghasempour, C. Yeh, R. Shrestha, Y. Amarasinghe, D. Mittleman, and E. Knightly, "LeakyTrack: Non-coherent single-antenna nodal and environmental mobility tracking with a leaky-wave antenna," in *Proc. 18th ACM SenSys*, 2020, pp. 1–13.

[24] S. Darbha, S. Konduri, and P. R. Pagilla, "Benefits of V2V communication for autonomous and connected vehicles," *IEEE Trans. Intell. Transp. Syst.*, vol. 20, no. 5, pp. 1954–1963, May 2019.

[25] Y. Heng, J. G. Andrews, J. Mo, V. Va, A. Ali, B. L. Ng, and J. C. Zhang, "Six key challenges for beam management in 5.5G and 6G systems," *IEEE Commun. Mag.*, vol. 59, no. 7, pp. 74–79, July 2021.

[26] V. Va, H. Vikalo, and R. W. Heath, "Beam tracking for mobile millimeter wave communication systems," in *IEEE Global Conf. Signal and Inf. Process. (GlobalSIP)*, 2016, pp. 743–747.

[27] S. Jayaprakasam, X. Ma, J. W. Choi, and S. Kim, "Robust beam-tracking for mmwave mobile communications," *IEEE Commun. Letters*, vol. 21, no. 12, pp. 2654–2657, Dec. 2017.

[28] J. Zhao, F. Gao, W. Jia, S. Zhang, S. Jin and H. Lin, "Angle domain hybrid precoding and channel tracking for millimeter wave massive MIMO systems," *IEEE Trans. Wireless Commun.*, vol. 16, no. 10, pp. 6868–6880, Oct. 2017.

[29] X. Gao, L. Dai, Y. Zhang, T. Xie, X. Dai, and Z. Wang, "Fast channel tracking for terahertz beamspace massive MIMO systems," *IEEE Trans. Veh. Technol.*, vol. 66, no. 7, pp. 5689–5696, 2017.

[30] J. Tan and L. Dai, "Wideband beam tracking in THz Massive MIMO systems," *IEEE J. Sel. Areas Commun.*, vol. 39, no. 6, pp. 1693–1710, June 2021.

[31] Z. Lin, L. Wang, B. Tan, and X. Li, "Spatial-spectral Terahertz Networks," *IEEE Trans. Wireless Commun.*, vol. 21, no. 6, pp. 3881-3892, June 2022.

[32] M. Alzard, S. Althunibat, K. Umebayashi and N. Zorba, "Resource allocation in THz-based subcarrier index modulation systems for mobile users," *IEEE GLOBECOM*, 2021, pp. 1-6.

[33] H. Sarieddeen, M.-S. Alouini, and T. Y. Al-Naffouri, "An overview of signal processing techniques for terahertz communications," *Proc. IEEE*, vol. 109, no. 10, pp. 1628–1665, Oct. 2021.

[34] S. M. Kay, *Fundamentals of Statistical Signal Processing: Estimation Theory*, vol. 1. Englewood Cliffs, NJ, USA: Prentice-Hall, 1998.

[35] S. Julier, J. Uhlmann, and H. F. Durrant-Whyte, "A new method for the nonlinear transformation of means and covariances in filters and estimators," *IEEE Trans. Automat. Contr.*, vol. 45, no. 3, pp. 477–482, Mar. 2000.

[36] E. A. Wan and R. van der Merwe, *The Unscented Kalman Filter*, John Wiley & Sons, Inc., 2001.

[37] T. Lefebvre, H. Bruyninckx, and J. D. Schuttere, "Comment on "a new method for the nonlinear transformation of means and covariances in filters and estimators"," *IEEE Trans. Automat. Contr.*, vol. 47, no. 8, pp. 1406–1408, Aug. 2002.

[38] A. Sutinjo, M. Okoniewski, and R. H. Johnston, "Radiation from fast and slow traveling waves," *IEEE Antennas Propag. Mag.*, vol. 50, no. 4, pp. 175–181, Aug. 2008.

[39] D. R. Jackson, C. Caloz, and T. Itoh, "Leaky-wave antennas," *Proc. IEEE*, vol. 100, no. 7, pp. 2194–2206, July 2012.

[40] Y. Yu, R. Jiang and X. Qu, "A modified full velocity difference model with acceleration and deceleration confinement: Calibrations, validations, and scenario analyses," *IEEE Intell. Transp. Syst. Mag.*, vol. 13, no. 2, pp. 222-235, 2021.

[41] R. K. Jain, D. W. Chiu, and W. R. Hawe, "A quantitative measure of fairness and discrimination for resource allocation in shared systems," Tech. Rep., Digital Equipment Corporation, DEC-TR-301, 1984.

[42] W. Yu, "Sum-capacity computation for the gaussian vector broadcast channel via dual decomposition," *IEEE Trans. Inf. Theory*, vol. 52, no. 2, pp. 754–759, Feb. 2006.

[43] M. Kobayashi and G. Caire, "An iterative water-filling algorithm for maximum weighted sum-rate of Gaussian MIMO-BC," *IEEE J. Sel. Areas Commun.*, vol. 24, no. 8, pp. 1640–1646, Aug. 2006.

[44] M. Grant, S. Boyd, and Y. Ye. (2008). *CVX: MATLAB Software for Disciplined Convex Programming. [Online].* Available:. [Online]. Available: https://web.stanford.edu/~boyd/papers/pdf/disc_cvx_prog.pdf

[45] S. H. Han and J. H. Lee, "An overview of peak-to-average power ratio reduction techniques for multicarrier transmission," *IEEE Wireless Commun.*, vol. 12, no. 2, pp. 56–65, Apr. 2005.

[46] J. Kokkoniemi, J. Lehtomäki, and M. Juntti, "A line-of-sight channel model for the 100-450 gigahertz frequency band," *EURASIP J. Wireless Com Network*, pp. 1–15, Apr. 2021.

Zheng Lin is a postgraduate at the Department of Electrical Engineering, Fudan University. His research interest focuses on the Terahertz networks.

Lifeng Wang is a faculty member at the Department of Electrical Engineering, Fudan University. He received the Ph.D. degree in Electrical Engineering from the Queen Mary University of London, U.K. He was a Research Associate with the Department of Electronic and Electrical Engineering, University College London (UCL), U.K. His research interests include 5G/6G systems, ITS and information security. He received the Exemplary Editor Certificates of the IEEE Communications Letters in 2016-2018. Currently he serves as an associate editor in the IEEE Transactions on Intelligent Transportation Systems.

Jie Ding received her B.Eng. degree in automation from Harbin Engineering University, China in 2012 and Ph.D. degree in electrical and electronic engineering from Nanyang Technological University, Singapore in 2018. She was a Scientist in Institute for Infocomm Research (I2R), Agency for Science, Technology and Research (A*STAR), Singapore, from July 2018 to August 2019. Since September 2019, she has been with the Electronic Engineering Department, Fudan University, P.R. China, where she is currently a pre-tenure associate professor. Her research interests include machine learning, pattern recognition, control & optimization and complex networks.

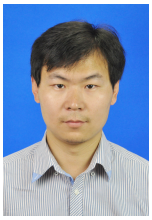

Yuedong Xu is a Professor with School of Information Science and Technology, Fudan University, China. He received B.S. degree from Anhui University in 2001, M.S. degree from the Huazhong University of Science and Technology in 2004, and Ph.D. degree from The Chinese University of Hong Kong in 2009. From 2009 to 2012, he was a Postdoctoral Researcher with INRIA Sophia Antipolis and Universit d'Avignon, France. He received the French MENRT fellowship in 2009 and the OKAWA Foundation research grant in 2019. His areas of interests include network performance evaluation, multimedia networking and distributed machine learning. He has published more than 30 papers in premier conferences and journals including ACM Mobisys, CoNEXT, Mobihoc, IEEE Infocom and IEEE/ACM ToN, IEEE JSAC.

Bo Tan received the B.Sc. and M.Sc. degrees in communications engineering from the Beijing University of Posts and Telecommunications in 2004 and 2008, respectively, and the PhD degree from the Institute for Digital Communications, The University of Edinburgh, U.K., in 2013. From 2012 to 2016, he was the postdoctoral researcher at University College London and the University of Bristol, UK. From 2017 to 2018, he was the lecturer at Coventry University, UK. Since 2019, he has been an Assistant Professor with Tampere University, Finland. His research interests include radio signal processing, wireless communications systems, joint sensing-communications design, machine learning of multiple modal sensing data fusion for human activity recognition, sensing and positioning for intelligent machines.